PCCP

Accepted Manuscript

ROYAL SOCIETY OF CHEMISTRY

www.rsc.org/pccp

DFT study on endohedral and exohedral B_{38} fullerenes: M@B_{38} (M=Sc, Y, Ti) and M&B_{38} (M=Nb, Fe, Co, Ni)

Qi Liang Lu,[a,*] Qi Quan Luo,[b] Yi De Li,[a] Shou Guo Huang[a]

The structures, stabilities and electronic properties of endohedral and exohedral B_{38} fullerenes with transition metal atoms (M=Sc, Y, Ti, Nb, Fe, Co, Ni) are studied using all-electron density functional theory. M@B_{38} (M = Sc, Y, Ti) possess endohedral structures as their lowest energy structures, while Nb, Fe, Co and Ni atoms favor to coordinate B_{38} fullerene in an exohedral manner. Sizable HOMO-LUMO gaps and large binding energies imply the viability of M@B_{38} to experimental realization. The distributions of electron density and frontier orbitals are analyzed in detail. The analysis of vertical ionization potential and vertical electron affinity indicates M@B_{38} is good electron acceptor and bad electron donor.

1 Introduction

After the discovery of C_{60} buckyball, the fullerene like nanostructures have received much attention due to their novel physical and chemical properties as well as their potential application in building blocks for nanomaterials. As the nearest neighbor of carbon in the periodic table, all boron fullerene analogues have been pursued in the past few years since the pioneering theoretical prediction of B_{80} cage in 2007 [1-16]. However, subsequently evidences for boron fullerenes are scarce. Recent studies have revealed that core-shell structures are more energetically favorable in the size range with $n \geq 68$ [17-20]. While for smaller sized B_n clusters, studies have

[a] *School of Physics and Material Science, Anhui University, Hefei 230601, Anhui, P. R. China*
E-mail: qllufd@vip.sina.com
[b] *Department of Chemical Physics, University of Science and Technology of China, Hefei 230026, Anhui, P. R. China*

shown that planar or quasi-planar structures are stable even at sizes of n=30 and 36 [21-23]. The 2D-to-3D structural transition occurred at approximately range from 20 to 68 atoms. Therefore, the search for boron fullerene is limited to these medium-size clusters. Remarkable progress has been made on the boron fullerene recently. Zhai et al. [24] observed an all-boron fullerene-like cage cluster B_{40}^- by photoelectron spectroscopy. Joint experimental and theoretical investigations confirmed that the structure of $B_{40}^{-/0}$ is fullerene-like cage. Lv et al. [25] reported an unusually stable B_{38} fullerene analogue through first-principles swarm structure searching calculations. It adopts a D_{2d} symmetry with four hexagonal holes and a large energy gap (~2.25 eV) as well as high aromaticity.

Interest in stable fullerenes is to search for novel building blocks for nanostructures. Encapsulating one or more metal atoms inside a cage has often been used to functionalize the fullerene. Endohedral metallofullerene La@C_{60} was immediately synthesized after the discovery of C_{60} fullerene [26]. Various endohedral fullerenes were subsequently reported different atoms or clusters inside the cage [27-36]. Similarly, discovery of these boron fullerenes will pave the way of borospherene chemistry. Very recently, the endohedral borospherene M@B_{40} encapsulated with alkaline-earth atoms (M=Ca, Sr, Li) [37, 38] and transition metal atoms (M=Sc, Y, La) [39] were studied using density functional theory. Most recently, Zhang et al. demonstrated the stabilization of B_{24} cages by transition metal encapsulation [40]. The mean spherical diameter of B_{38} is 5.85 Å, which is 1.25 Å smaller than that of C_{60} (7.1 Å). The space is large enough to accommodate some atomic species inside to form

endohedral borospherene M@B_{38} as their most stable structures. On the other hand, the four hexagonal holes on the surface of B_{38} suggest the possibility to coordinate these atoms in an exohedral manner. Both exohedral and enohedral complexes are intriguing for theory and application. Inspired by these studies on B_{40}, we will theoretically explore a series of exohedral and enohedral B_{38} fullerene with transition metal atoms (M=Sc, Y, Ti, Nb, Fe, Co, Ni). We will find the possibility to encapsulate metal atoms inside B_{38}.

2 Computational methods

All calculations are carried using the Dmol3 code based on density functional theory (DFT) [41]. In the Dmol3 electronic structure calculations, all electron treatments and double numerical polarized (DNP) [42] basis sets are selected. The generalized gradient approximation (GGA) [43] with the Perdew–Burke–Ernzerh (PBE) functional is employed for the exchange correlation potential [44]. The real-space global cutoff radius is set at 5.5 Å. Self-consistent field calculations on the total energy and electron density are performed with a convergence criterion of 10^{-5} a. u. We use a convergence criterion of 0.004 Hartree/Å on force, 0.005 Å on displacement, and 2 x 10^{-5} Hartree on the total energy in geometry optimization. All calculations are spin unrestricted, and the smearing is set as 0.005 Hartree to ensure convergence.

For B_{38} fullerene, the calculated bond length of hexagon holes (1.647 Å and 1.757 Å, respectively) and average binding energy (5.73 eV/atom) are good agreement with those of Ref. 25 (1.650 Å, 1.753 Å and 5.41 eV/atom) which were calculated with the

PAW method. Isomer quasi-planar structure is less stable than the fullerene analogue by 0.654 eV. This result is consistent with those of Ref. 25 (0.21 eV) and Ref. 45 (0.38 eV) at the PBE0/6-331G(d) level of theory.

3 Results and discussions

The structure of B_{38} fullerene is highly symmetric and consists of four hexagon holes [25]. One pair of hexagon holes is respectively connected with four hexagons (H-1). The other pair of hexagon holes is surrounded by two pentagons (H-2). The topologies are shown in Fig. 1. Metal atoms may coordinate the four hexagonal holes on the surface of B_{38}. Meanwhile, metal atoms can be inside the cage. Therefore, several different locations are available for these atoms. Moreover, higher level of theory shown that fullerene structure and quasi-planar structure are almost degenerate in energy [45]. Structural transition may occurs after doping with other atoms. There are two hexagon holes that metal atoms can be doped in the quasi-planar structure (see Fig.1). All possible topologies as candidate structures are further optimized with the Dmol3 code.

The relative stability of these metal atoms doped B_{38} are listed in Table 1. The most stable structures of endohedral or exohedral B_{38} fullerenes are shown in Figure 2. Results clearly show that $M@B_{38}$ (M=Sc, Y, Ti) possess endohedral structures as their lowest energy configurations, in which the metal atom reside in the cage. In $Y@B_{38}$, Y atom is almost at the center position of the cage. For comparison, Sc and Ti atoms slightly deviate from the cage center by about 0.68 and 0.98 Å, respectively. Sc is close to the hexagonal ring of the H-2 site, whereas Ti approach the center of H-1

hexagon hole. The smallest M-B bond length is 2.39, 2.66 and 2.27 Å for M=Sc, Y and Ti, respectively. Whereas for M= Nb, Fe, Co, Ni dopants with smaller atomic radii, B_{38} fullerene coordinate metal atoms in an exohedral manner (M&B_{38}), in which Nb, Fe and Co prefer to face-capping on the H-2 hexagon hole. Fe and Co form an almost perfectly filled hexagon hole on the surface of B_{38} cage. Furthermore, small energy difference can be found between Nb&B_{38} and Nb@B_{38}. In contrast with its counterparts, Ni atom occupy a H-1 hexagon hole in a face-capping configuration. The nearest M-B distances are 2.16, 1.96, 1.96 and 1.98 Å for M=Nb, Fe, Co and Ni, respectively. Large binding energies of the four transition metal atoms can be found from Table 1, suggesting the structural stability after doping. All the results show that the larger size of Sc, Y and Ti atoms is ideal match for the B_{38} cage in the endohedral manner. The transition metal atoms move from inside to outside of the B_{38} cage with decreasing atomic radii. From Table 1, we can also see that the metal doped quasi-planar structures are still not energetically favorable. Sc, Y, Ti and Nb atom favors to occupy the B hexagon holes of the structure. While Fe, Co and Ni prefer to face-capping on the A hexagon hole. The increased energy difference can be found between fullerene and quasi-planar structure for M=Sc, Ti, Fe, Co, Ni. Doping with metal atoms may favor to isolating B_{38} fullerene. But for M=Y and Nb, the energy difference becomes smaller.

We focus on the properties of endohedral M@B_{38} (M=Sc, Y, Ti) structures. The encapsulation process of metal atoms into the cage is an exothermic process that yields binding energies of Sc, Y and Ti atoms are 5.22, 5.54 and 6.07 eV with respect

to $M+B_{38}=MB_{38}$ (See Table 1). For comparison, binding energies of Sc, Y for experimentally abundant $Sc@C_{82}$-$C_{2v}(9)$ [46] and $Y@C_{82}$-$C_{2v}(9)$ [47] are 5.24 and 5.80 eV, respectively, at the present level of the theory. This magnitude indicates substantial interaction between the metal atoms and the cage as well as considerable stabilization of these endohedral boron fullerenes. Mulliken population analysis shows that atomic charges of Sc, Y and Ti are -0.20, -0.42 and -0.28e, implying substantial charge transfers from the outer cage to the metal atoms. The changes in charge can be identified by visualisation of the spatially deformed charge distribution in these endohedral fullerenes, which is defined as the total charge density minus the density of the isolated atoms. The electronic character of $M@B_{38}$ at an iso-value of 0.15 $e/Å^3$ are displayed in Figure 3. It clearly shows that a large amounts of difference charges are on the B_{38} cage and mainly distributed on the four hexagonal rings. It means that there is covalency in B-B interactions.

Figure 4 shows the charge density of HOMO and LUMO of these endohedral boron fullerenes. The HOMO of $Sc@B_{38}$ and $Ti@B_{38}$ is predominately delocalized inside the cage and mainly distributed in both sides of Sc and Ti atom. While for $Y@B_{38}$, it is mainly localized on one couple of hexagonal rings of the boron cage. The contribution of Y atom to the HOMO is very small. The LUMO orbital of these $M@B_{38}$ mainly locate on the outer cage and a quite amount of charges are distributed on the two boron atoms filling one couple of pentagon rings. Sc, Y and Ti atoms carry relatively small amount of the charge density. The HOMO-LUMO gaps of $Sc@B_{38}$, $Y@B_{38}$ and $Ti@B_{38}$ are 0.58, 0.45 and 0.78 eV, respectively, much smaller than that

of the pristine B_{38} (The value is 1.25 eV at the present level of the theory. Ref. [25] give the result of 2.25 eV).

The introduction of transition metal atoms can produce spin density and magnetism on the M@B_{38} systems. Both Sc@B_{38} and Ti@B_{38} are nonmagnetic. Y@B_{38} carries net magnetic moment by only 0.006μ_B. Such small moment is safe to say Y@B_{38} is virtually nonmagnetic. The quenched magnetism results from delocalization of the *d*-electron, dues to the orbital hybridization between *sp* electrons of B_{38} and *d* electrons of transition metal atoms.

The calculated vertical ionization potential (VIP), vertical electron affinity (VEA) of Sc@B_{38}, Y@B_{38} and Ti@B_{38} are 6.05, 5.96 and 6.36 eV as well as 2.47, 2.39 and 2.43 eV, respectively. It suggests that these endohedral boron fullerenes have good electron accepting capacity. Studies shown that hollow fullerene are good electron acceptor materials [48]. The combination of fullerene and some organometallic molecule can provide nanostructures for opto-electronic devices of the p (an electron acceptor)-n (an electron donor) junction type [49-51]. It is interesting to discuss the donor-acceptor properties of these endohedral boron fullerenes. A model was proposed to evaluate accepting and donating capacity of a system [52-55]. The accept and donate electron power can be defined as

$$\omega^{+} = \frac{(VIP + 3VEA)^2}{16(VIP - VEA)}$$

$$\text{and } \omega^{-} = \frac{(3VIP + VEA)^2}{16(VIP - VEA)}.$$

F and Na atoms are chosen for reference as a good electron acceptor and donor.

An electron acceptance index can be defined as $R_a = \omega^+ / \omega_F^+$. $R_a > 1$ means M@B_{38} has better accepting power than F atom. An electron donation index is defined as $R_d = \omega^- / \omega_{Na}^-$ [53, 54]. $R_d > 1$ means M@B_{38} is a worse electron donor than Na atom. The VIP and VEA of F atom obtained at the same level of theory are 17.84 eV and 2.84 eV. Corresponding values of Na atom are 5.26 eV and 0.28 eV, respectively. The obtained R_a = 1.09, 1.04 and 1.02, whereas R_d = 2.29, 2.22 and 2.27 for Sc@B_{38}, Y@B_{38} and Ti@B_{38}, respectively. These data show that M@B_{38} (M = Sc, Y, Ti) are all good electron acceptor and bad electron donor, indicate that all of them are stable against oxidation.

4 Conclusions

In summary, exohedral and enohedral B_{38} fullerene with transition metal atoms (M = Sc, Y, Ti, Nb, Fe, Co, Ni) were explored by means of DFT calculations. Results shown that M@B_{38} (M = Sc, Y, Ti) possess endohedral structures as their lowest energy structures, while Nb, Fe, Co and Ni atoms favor to coordinate B_{38} fullerene in an exohedral manner. Sc@B_{38}, Y@B_{38} and Ti@B_{38} hold sizable HOMO-LUMO gaps and large binding energies imply their promise for experimental realization. Sc, Y and Ti atoms are all negatively charged. Sc@B_{38}, Y@B_{38} and Ti@B_{38} are all nonmagnetic. The analysis of VIP and VEA indicates M@B_{38} are good electron acceptor and bad electron donor. These endohedral boron fullerenes have additional properties arising from metal–cage interactions. This will broaden their applications in catalyst, medicine, electronics and photovoltaics. For example, the combination of endohedral fullerene and some organometallic molecule can provide nanostructures for

opto-electronic devices of the p (an electron acceptor)-n (an electron donor) junction type. Recently, Ref. 38 shown that endohedral boron fullerenes $Li@B_{40}$ is an efficient sorbent for CO_2 capture and separation. It is expected that the unique properties of endohedral boron fullerenes should be further investigated.

References

1 N. G. Szwacki, A. Sadrzadeh and B. I. Yakobson, *Phys. Rev. Lett.*, 2007, **98**, 166804.

2 N. G. Szwacki, *Nanoscale Res. Lett.*, 2008, **3**, 49–54.

3 Q. B. Yan, X. L. Sheng, Q. R. Zheng, L. Z. Zhang and G. Su, *Phys. Rev. B*, 2008, **78**, 201401.

4 R. R. Zope, T. Baruah, K. C. Lau, A. Y. Liu, M. R. Pederson and B. I. Dunlap, *Phys. Rev. B*, 2009, **79**, 161403.

5 B. Shang, L. F. Yuan, X. C. Zeng and J. Yang, *J. Phys. Chem. A*, 2010, **114**, 2245–2249.

6 L. Wang, J. Zhao, F. Li and Z. Chen, *Chem. Phys. Lett.*, 2010, **501**, 16–19.

7 X. Q. Wang, *Phys. Rev. B*, 2010, **82**, 153409.

8 N. G. Szwacki and C.J. Tymczak, *Chem. Phys. Lett.*, 2010, **494**, 80–83.

9 C. Özdoğan, S. Mukhopadhyay, W. Hayami, Z. B. Güenç, R. Pandey and I. Boustani, *J. Phys. Chem. C*, 2010, **114**, 4362–4375.

10 R. R. Zope and T. Baruah, *Chem. Phys. Lett.*, 2011, **501**, 193–196.

11 W. Hayami and S. Otani, *J. Phys. Chem. A*, 2011, **115**, 8204–8207.

12 J. T. Muya, G. Gopakumar, M. T. Nguyen and A. Ceulemans, *Phys. Chem. Chem. Phys.*, 2011, **13**, 7524–7533.

13 S. Polad and M. Ozay, Phys. *Chem. Chem. Phys.*, 2013, **15**, 19819–19824.

14 J. T. Muya, E. Lijnen, M. T. Nguyen and A. Ceulemans, *Chem. Phys. Chem.*, 2013, **14**, 346–363

15 D. L. V. K. Prasad and E. D. Jemmis, *Phys. Rev. Lett.*, 2008, **100**, 165504.

16 P. Pochet, L. Genovese, S. De, S. Goedecker, D. Caliste, S. A. Ghasemi, K. Bao and T. Deutsch, *Phys. Rev. B*, 2011, **83**, 081403.

17 F. Li, P. Jin, D. E. Jiang, L. Wang, S. B. Zhang, J. Zhao and Z. Chen, *J. Chem. Phys.*, 2012, **136**, 074302.

18 J. Zhao, L. Wang, F. Li and Z. Chen, *J. Phys. Chem. A*, 2010, **114**, 9969–9972.

19 H. Li, N. Shao, B. Shang, L. F. Yuan, J. Yang and X. C. Zeng, *Chem. Commun.*, 2010, **46**, 3878–3880.

20 S. De, A. Willand, M. Amsler, P. Pochet, L. Genovese and S. Goedecker, *Phys. Rev. Lett.*, 2011, **106**, 225502–225505

21 T. B. Tai, L. V. Duong, H. T. Pham, D. T. T. Mai and M. T. Nguyen, *Chem. Commun.*, 2014, **50**, 1558–1560.

22 Z. A. Piazza, H. S. Hu, W. L. Li, Y. F. Zhao, J. Li and L. S. Wang, *Nat. Commun.*, 2014, **5**, 3113–3117.

23 W. L. Li, Q. Chen, W. J. Tian, H. Bai, Y. F. Zhao, H. S. Hu, J. Li, H. J. Zhai, S. D. Li, L. S. Wang, *J. Am. Chem. Soc.*, 2014, **136**, 12257–12260.

24 H. J. Zhai, Y. F. Zhao, W. L. Li, Q. Chen, H. Bai, H. S. Hu, Z. A. Piazza, W. J. Tian, H. G. Lu, Y. B. Wu, Y. W. Mu, G. F. Wei, Z. P. Liu, J. Li, S. D. Li and L. S. Wang, *Nat. Chem.*, 2014, **6**, 727–731.

25 J. Lv, Y. Wang, L. Zhu and Y. Ma, *Nanoscale*, 2014, **6**, 11692–11696.

26 J. R. Heath, S. C. O._Brien, Q. Zhang, Y. Liu, R. F. Curl, H. W. Kroto, F. K. Tittel and R. E. Smalley, *J. Am. Chem. Soc.*, 1985, **107**, 7779–7780.

27 Z. Wan, J. F. Christian and S. L. Anderson, *Phys. Rev. Lett.*, 1992, **69**, 1352–1355.

28 P. Weis, R. D. Beck, G. Brauchle and M. M. Kappes, *J. Chem. Phys.*, 1994, **100**, 5684–5695.

29 Y. Kubozono, H. Maeda, Y. Takabayashi, K. Hiraoka, T. Nakai, S. Kashino, S. Emura, S. Ukita and T. Sogabe, *J. Am. Chem. Soc.*, 1996, **118**, 6998 – 6999.

30 M. Saunders, R. J. Cross, H. A. Jiménez-Vázquez, R. Shimshi and A. Khong, *Science*, 1996, **271**, 1693 – 1697.

31 T. A. Murphy, T. Pawlik, A. Weidinger, M. Höhne, R. Alcala and J. M. Spaeth, *Phys. Rev. Lett.*, 1996, **77**, 1075 – 1078.

32 C. R. Wang, T. Kai, T. Tomiyama, T. Yoshida, Y. Kobayashi, E. Nishibori, M. Takata, M. Sakata and H. Shinohara, *Nature*, 2000, **408**, 426–427.

33 S. Stevenson, G. Rice, T. Glass, K. Harich, F. Cromer, M. R. Jordan, J. Craft, E. Hadju, R. Bible, M. M. Olmstead, K. Maitra, A. J. Fisher, A. L. Balch and H. C. Dorn. *Nature,* 1999, **401**, 55–57.

34 C. R. Wang, T. Kai, T. Tomiyama, T. Yoshida, Y. Kobayashi, E. Nishibori, M. Takata, M. Sakata and H. Shinohara, *Angew. Chem. Int. Ed.*, 2001, **40**, 397–399.

35 S. Stevenson, M. A. Mackey, M. A. Stuart, J. P. Phillips, M. L. Easterling, C. J. Chancellor, M. M. Olmstead and A. L. Balch, *J. Am. Chem. Soc.*, 2008, **130**, 11844–11845.

36 M. Saunders, R. J. Cross, H. A. Jiménez-Vázquez, R. Shimshi and A. Khong, *Science*, 1996, **271**, 1693–1697.

37 H. Bai, Q. Chen, H. J. Zhai and S. D. Li, Angew. Chem. Int. Ed., 2015, **54**,

941-945.

38 G. Gao, F. Ma, Y. Jiao, Q. Sun, Y. Jiao, E. Waclawik and A. Du, *Comp. Mater. Sci*., 2015, **108**, 38–41.

39 P. Jin, Q. Hou, C. Tang and Z. Chen, *Theor. Chem. Acc.*, 2015, **134**, 13.

40 J. Lv, Y. Wang, L. Zhang, H. Lin, J. Zhao and Y. Ma, *Nanoscale*, 2015, **7**, 10482-10489.

41 Dmol3 is a density functional theory (DFT) package distributed by MSI. B. Delley, *J. Chem. Phys.*, 1990, **92**, 508-517.

42 B. Delley, *J. Chem. Phys*., 2000, **113**, 7756-7764.

43 J. P. Perdew and Y. Wang, *Phys. Rev. B*, 1992, **45**, 13244-13249.

44 J. P. Perdew, K. Burke and M. Ernzerhof, *Phys. Rev. Lett.*, 1996, **77**, 3865-3868.

45 T. B. Tai and M. T. Nguyen, *Nanoscale*, 2015, **7**, 3316-3317.

46 E. Nishibori, M. Takata, M. Sakata, M. Inakuma and H. Shinohara, *Chem. Phys. Lett.*, 1998, **298**,79–84.

47 M. Takata, B. Umeda, E. Nishibori, M. Sakata, Y. Saito, M. Ohno and H. Shinohara, *Nature*, 1995, **377**, 46–49.

48 F. Langa and J. F. Nierengarten, *Fullerenes: Principles and Applications*, 2007, Oxford: Royal Society of Chemistry.

49 D. M. Guldi, B. M. Illescas, C. M. Atienza, M. Wielopolski and N. Martín, *Chem. Soc. Rev.*, 2009, **38**, 1587–1597.

50 G. Bottari, G. de la Torre, D. M. Guldi and T. Torres, *Chem. Rev.*, 2010, **110**, 6768-6816.

51 M. Quintiliani, A. Kahnt, T. Wöfle, W. Hieringer, P. Vázquez, A. Görling, D. M. Guldi and T. Torres, *Chem. Eur. J.*, 2008, **14**, 3765–3775.

52 E. Ramos, B. M. Monroy, J. C. Alonso, L. E. Sansores, R. Salcedo and A. Martínez, *J. Phys. Chem. C*, 2012, **116**, 3988–3994.

53 A. Martínez, M. A. Rodríguez-Gironés, A. Barbosa and M. Costas, *J. Phys. Chem. A*, 2008, **112**, 9037–9042.

54 A. Martínez and A. Galano, *J. Phys. Chem. C*, 2010, **114**, 8184–8191.

55 J. L. Gázquez, A. Cedillo and A. Vela, *J. Phys. Chem. A*, 2007, **111**, 1966–1970.

Figure and Table captions

Figure 1 The structure of B_{38} fullerene and quasi-planar. In fullerene, one hexagon hole is connected with four hexagons (H-1), and the other hole is surrounded by two pentagons (H-2). There are two hexagon holes A and B in quasi-planar.

Table 1 The relative energies of transition metal atoms doped B_{38}. The binding energy (E_b) of metal atom for the lowest energy structure with respect to $M+B_{38}=MB_{38}$. The energy unit is eV.

Figure 2 The most stable structures of endohedral or exohedral B_{38} fullerenes.

Figure 3 Deformation electron density of $Sc@B_{38}$, $Y@B_{38}$ and $Ti@B_{38}$ at an iso-value of 0.15 electron/ $Å^3$.

Figure 4 The charge density of HOMO and LUMO of $Sc@B_{38}$, $Y@B_{38}$ and $Ti@B_{38}$.

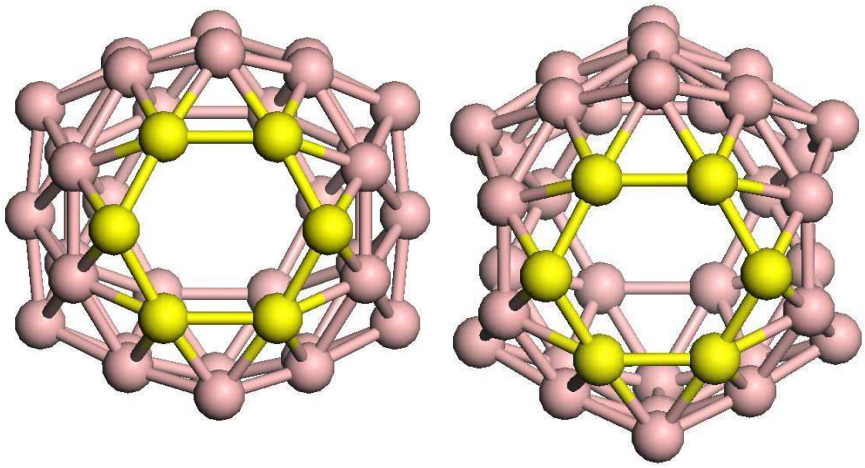

H-1 H-2

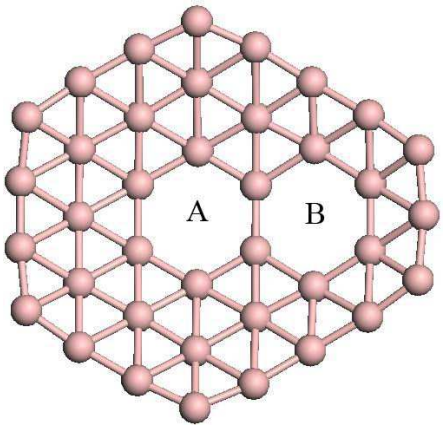

Figure 1 Q. L. Lu, et al.

	fullerene			quasi-planar		E_b
	H-1	H-2	endohedral	A	B	
Sc	0.61	1.17	0.00	1.43	0.72	5.22
Y	0.73	1.32	0.00	1.24	0.52	5.54
Ti	0.74	0.85	0.00	1.57	0.95	6.07
Nb	0.39	0.00	0.08	1.14	0.53	5.51
Fe	0.46	0.00	1.93	2.01	2.09	5.43
Co	0.17	0.00	1.87	1.60	2.02	6.36
Ni	0.00	0.08	1.94	1.51	1.81	6.43

Table 1 Q. L. Lu, et al.

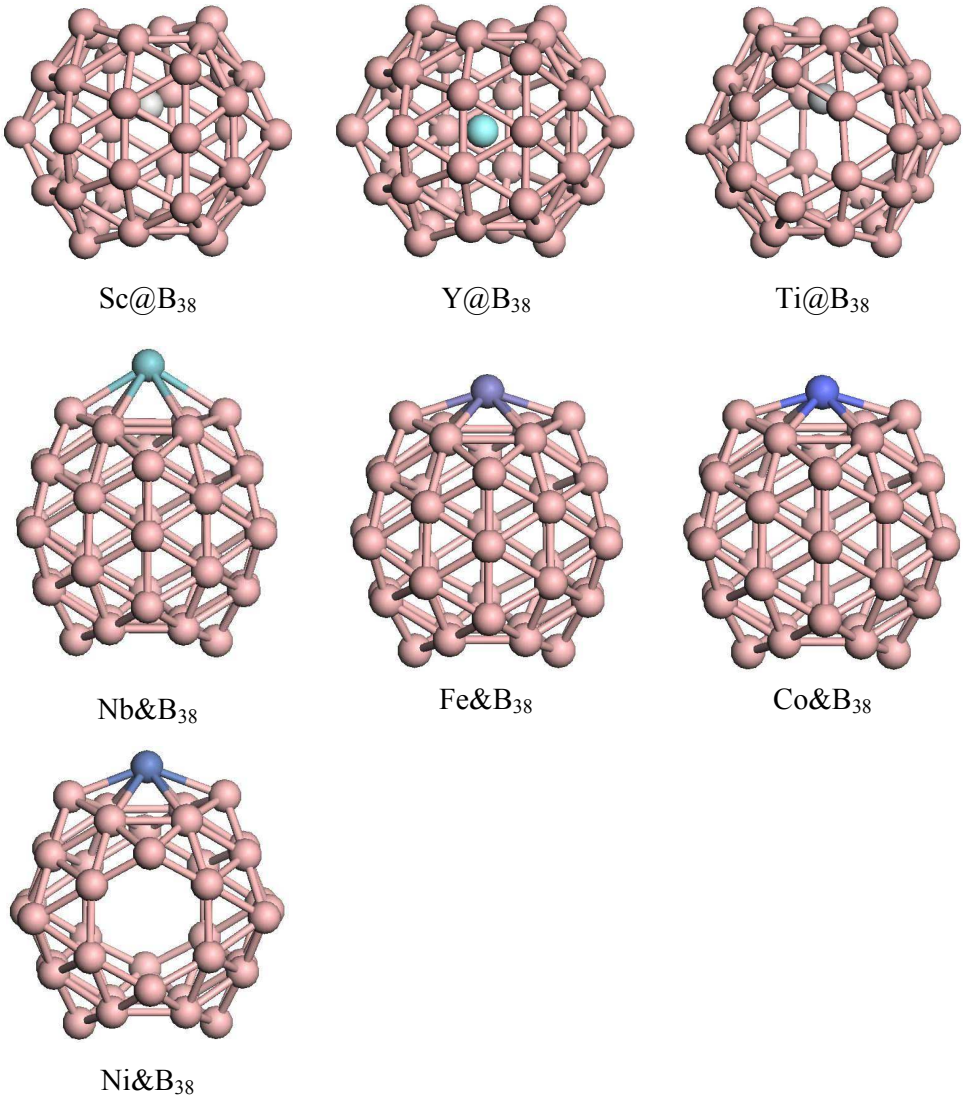

Figure 2 Q. L. Lu, et al.

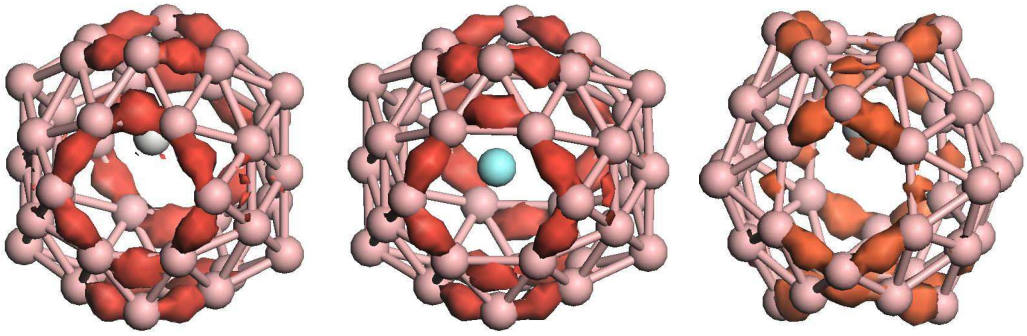

$Sc@B_{38}$ $Y@B_{38}$ $Ti@B_{38}$

Figure 3 Q. L. Lu, et al.

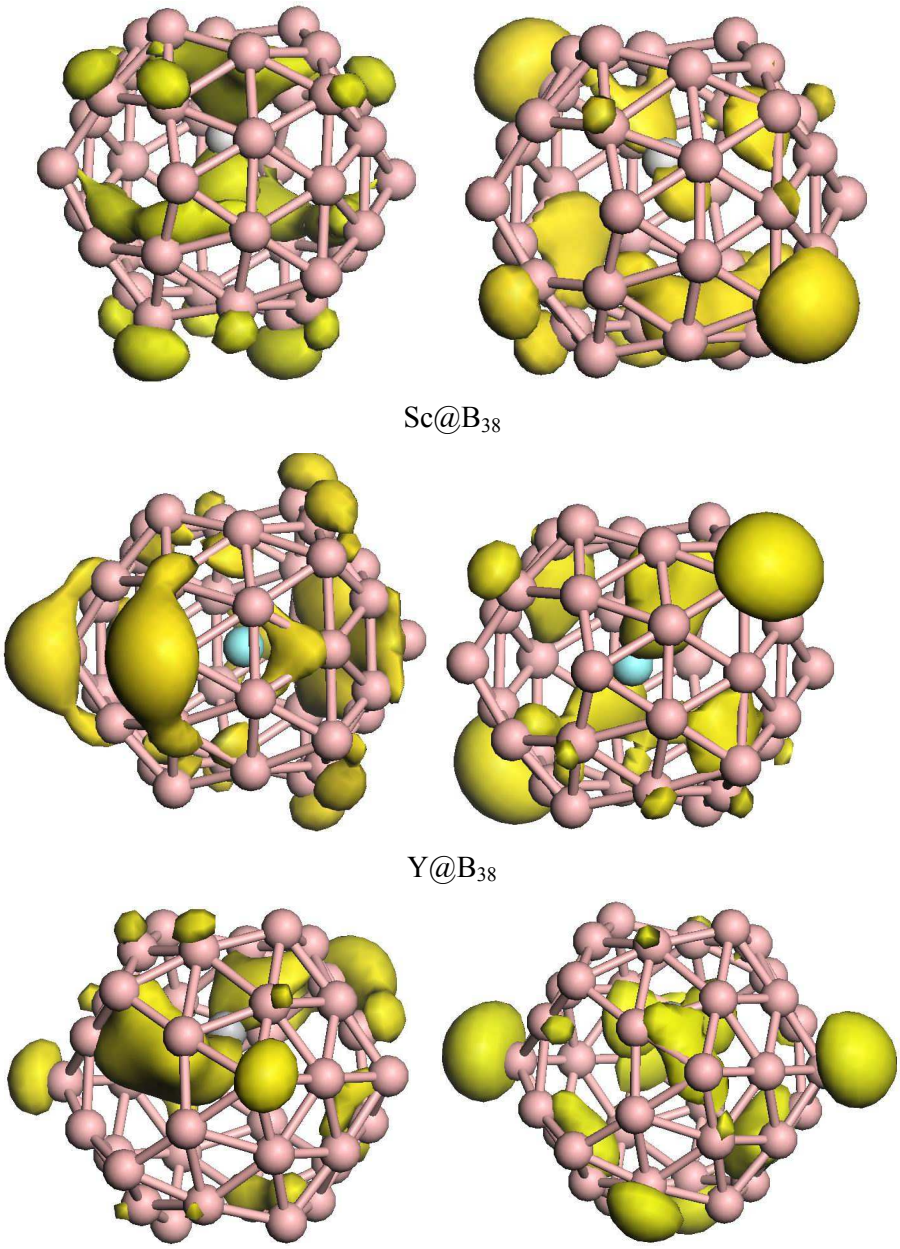

Figure 4 Q. L. Lu, et al.